Personal Verification using Palmprint and Hand Geometry Biometric

Ajay Kumar[1], David C. M. Wong[1], Helen C. Shen[1], Anil K. Jain[2]

[1] Department of Computer Science, Hong Kong University of Science and Technology, Clear Water Bay, Hong Kong.
{ajaykr, csdavid, helens}@cs.ust.hk

[2] Pattern Recognition and Image Processing Lab, Department of Computer Science and Engineering, Michigan State University, East Lansing, MI 48824.
jain@cse.msu.edu

Abstract. A new approach for the personal identification using hand images is presented. This paper attempts to improve the performance of palmprint-based verification system by integrating hand geometry features. Unlike other bimodal biometric systems, the users do not have to undergo the inconvenience of using two different sensors since the palmprint and hand geometry features can be acquired from the same image, using a digital camera, at the same time. Each of these gray level images are aligned and then used to extract palmprint and hand geometry features. These features are then examined for their individual and combined performances. The image acquisition setup used in this work is inherently simple and it does not employ any special illumination nor does it use any pegs to cause any inconvenience to the users. Our experimental results on the image dataset from 100 users confirm the utility of combining hand geometry features with those from palmprints using a simple image acquisition setup.

1 Introduction

Reliability in the personal authentication is key to the security in the networked society. Many physiological characteristics of humans, *i.e.*, biometrics, are typically time invariant, easy to acquire, and unique for every individual. Biometric features such as face, iris, fingerprint, hand geometry, palmprint, signature, *etc*. have been suggested for the security in access control. Most of the current research in biometrics has been focused on fingerprint and face [1]. The reliability of personal identification using face is currently low as the researchers today continue to grapple with the problems of pose, lighting, orientation and gesture [2]. Fingerprint identification is widely used in personal identification as it works well in most cases. However, it is difficult to acquire fingerprint features *i.e*. minutiae, for some class of persons such as manual laborers, elderly people, *etc*.. As a result, other biometric characteristics are receiving increasing attention. Moreover, additional biometric features, such as palmprints, can be easily integrated with the existing authentication system to provide enhanced level of confidence in personal authentication.

1.1 Prior work

Two kinds of biometric indicators can be extracted from the low-resolution† hand images; (i) palmprint features, which are composed of principal lines, wrinkles, minutiae, delta points, *etc*., and (ii) hand geometry features which include area/size of palm, length and width of fingers. The problem of personal verification using palmprint features has drawn considerable attention and researchers have proposed various methods [3]-[15]. One popular approach considers palmprints as textured images which are unique to every individual. Therefore, analysis of palmprint images using Gabor filters [3], wavelets [4], Fourier transform [5], and local texture energy [6] has been proposed in the literature. As compared to fingerprints, palmprints have a large number of creases. Wu *et al.* [7] have characterized these creases by directional line energy features and used them for palmprint identification. The endpoints of some prominent principal lines, *i.e*., the heart-line, head-line, and life-line are rotation invariant. Some authors [8]-[9] have used these endpoints

† High resolution hand images, of the order of 500 dpi, can also be used to extract fingerprint features. However, the database for such images will require large storage and computational requirements.

and midpoints for the registration of geometrical and structural features of principal lines for palmprint matching. Duta *et al.* [10] have suggested that the connectivity of extracted palm lines is not important. Therefore, they have used a set of feature points along the prominent palm lines, instead of extracted palm lines as in [9], to generate the matching score for palmprint authentication. The palmprint pattern also contains ridges and minutiae, similar to a fingerprint pattern. However, in palmprints the creases and ridges often overlap and cross each other. Therefore, Funda *et al.* [11] have suggested the extraction of local palmprint features, *i.e.*, ridges by eliminating the creases. However, this work [11] is only limited to the extraction of ridges, and does not go beyond its usage to support any success of these extracted ridges in the identification of palmprints. Chen *et al.* [12] have attempted to estimate palmprint crease points by generating a local gray level directional map. These crease points are connected together to isolate the crease in the form of line segments, which are used in the matching process. No details are provided in [12] to suggest the robustness of these partially extracted creases for the matching of palmprints. Some related work on palmprint verification also appears in [13] and [14]. A recent paper by Han *et al.* [15] uses morphological and Sobel edge features to characterize palmprints and trained a neural network classifier for their verification.

The palmrint authentication methods in [5]-[12] utilize inked palmprint images while the recent work in [4] and [15] have shown the utility of inkless palmprint images acquired from the digital scanner. However, some promising results on the palmprint images acquired from image acquisition systems using CCD based digital camera appear in [3] and [13].

The US patent office has issued several patents [16]-[19] for devices that measure hand geometry features for personal verification. Some related work using low-resolution digital hand images appears in [20] and [21]. These authors have used fixation pegs to restrict the hand movement and shown promising results. However, the results in [20]-[21] may be biased by the small size of the database and an imposter can easily violate the integrity of system by using fake hand [22].

1.2 Proposed system

The palmprint and hand geometry images can be extracted from a hand image in a single shot at the same time. Unlike other multibiometrics systems (*e.g.*, face and fingerprint [23], voice and face [24], *etc.*), a user does not have to undergo the inconvenience of passing through multiple sensors. Furthermore, the fraud associated with fake hand, in hand geometry based verification system, can be alleviated with the integration of palmprint features. This paper presents a new method of personal authentication using palmprint and hand geometry features that are simultaneously acquired from a single hand image. The block diagram of the proposed verification system is shown in figure 1. Hand images

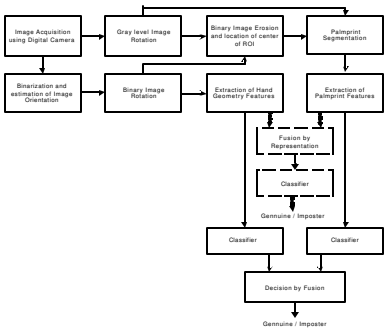

Figure 1: Block diagram of the personal verification system using palmprint and hand geometry

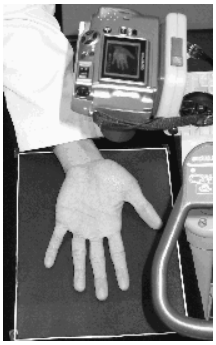

Figure 2 Acquisition of a typical image sample using digital camera.

of every user are used to automatically extract the palmprint and hand geometry features. This is achieved by first thresholding the images acquired from the digital camera. The resultant binary image is used to estimate the orientation of hand since in absence of pegs user does not necessarily align their hand in a preferred direction. The rotated binary image is used to compute hand geometry features. This image also serves to estimate the center of

palmprint from the residue of morphological erosion with a known structuring element (SE). This center point is used to extract the palmprint image of a fixed size, from the rotated gray level hand images. Each of these palmprint images are used to extract salient features. Thus the palmprint and hand geometry features of an individual are obtained from the same hand image. Two schemes for the fusion of features, fusion at the decision level and at the representation level, were considered. The decision level fusion gave better results as is detailed in section 5.

2. Image Acquisition & Alignment

Our image acquisition setup is inherently simple and does not employ any special illumination (as in [3]) nor does it use any pegs to cause any inconvenience to users (as in [20]). The Olympus C-3020 digital camera (1280 × 960 pixels) was used to acquire the hand images as shown in figure 2. The users were only requested to make sure that (i) their fingers do not touch each other and (ii) most of their hand (back side) touches the imaging table.

2.1 Extraction of hand geometry images

Each of the acquired images needs to be aligned in a preferred direction so as to capture the same features for matching. The image thresholding operation is used to obtain a binary hand-shape image. The threshold value is automatically computed using Otsu's method [25]. Since the image background is stable (black), the threshold value can be computed once and used subsequently for other images. The binarized shape of the hand can be approximated by an ellipse. The parameters of the best-fitting ellipse, for a given binary hand shape, is computed using the moments [26]. The orientation of the binarized hand image is approximated by the major axis of the ellipse and the required angle of rotation is the difference between normal and the orientation of image. As shown in figure 3, the binarized image is rotated and used for computing the hand geometry features. The estimated orientation of binarized image is also used to rotate gray-level hand image, from which the palmprint image is extracted as detailed in the next subsection.

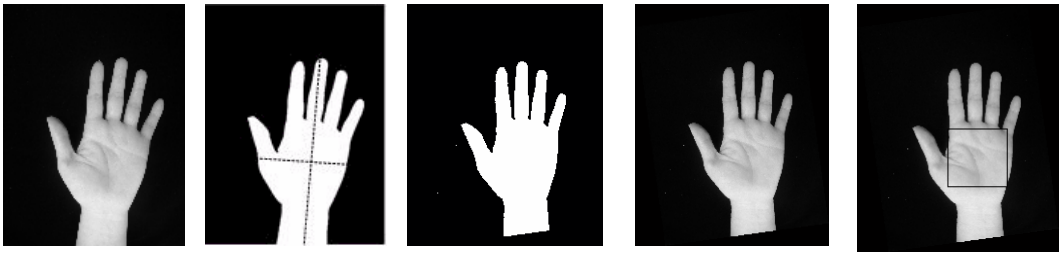

(a) (b) (c) (d) (e)

Figure 3. Extraction of two biometric modalities from the hand image, (a) captured image from the digital camera, (b) binarized image and ellipse fitting to compute the orientation (c) binary image after rotation, (d) gray scale image after rotation (e) ROI, *i.e.*, palmprint, extracted from the center of image in (c) after erosion.

2.2 Extraction of palmprint images

Every binarized hand-shape image is subjected to morphological erosion, with a known binary SE, to compute the region of interest, *i.e.*, the palmprint. Let R be the set of non-zero pixels in a given binary image and SE be the set of non-zero pixels, *i.e.*, structuring element. The morphological erosion is defined as

$$R \Theta SE = \{ g : SE_g \subseteq R \}, \quad (1)$$

where SE_g denotes the structuring element with its reference point shifted by g pixels. A square structuring element (SE) is used to probe the composite binarized image. The center of binary hand image after erosion, *i.e.*, the center of rectangle that can enclose the residue is determined. This center coordinates are used to extract a square palmprint region of fixed size as shown in figure 3.

2.3 Normalization of palmprints

The extracted palmprint images are normalized to have pre-specified mean and variance. The normalization is used to reduce the possible imperfections in the image due to sensor noise and non-uniform illumination. The method for normalization employed in this work is the same as suggested in [27] and is sufficient for the quality of acquired images in our experiments. Let the gray level at (x,y), in a palmprint image be represented by $I(x,y)$. The mean and variance of image, ϕ and ρ, respectively, can be computed from the gray levels of the pixels. The normalized image $I'(x, y)$ is computed using the pixel-wise operations as follows:

$$I'(x, y) = \begin{cases} \phi_d + \lambda & \text{if } I(x, y) > \phi \\ \phi_d - \lambda & \text{otherwise} \end{cases} \qquad \text{where } \lambda = \sqrt{\frac{\rho_d \{I(x, y) - \phi\}^2}{\rho}} \qquad (2)$$

where ϕ_d and ρ_d are the desired values for mean and variance, respectively. These values are pre-tuned according to the image characteristics, *i.e.*, $I(x,y)$. In all our experiments, the values of ϕ_d and ρ_d were fixed to 100. Figures 4 (a)-(b) show a typical palmprint image before and after the normalization.

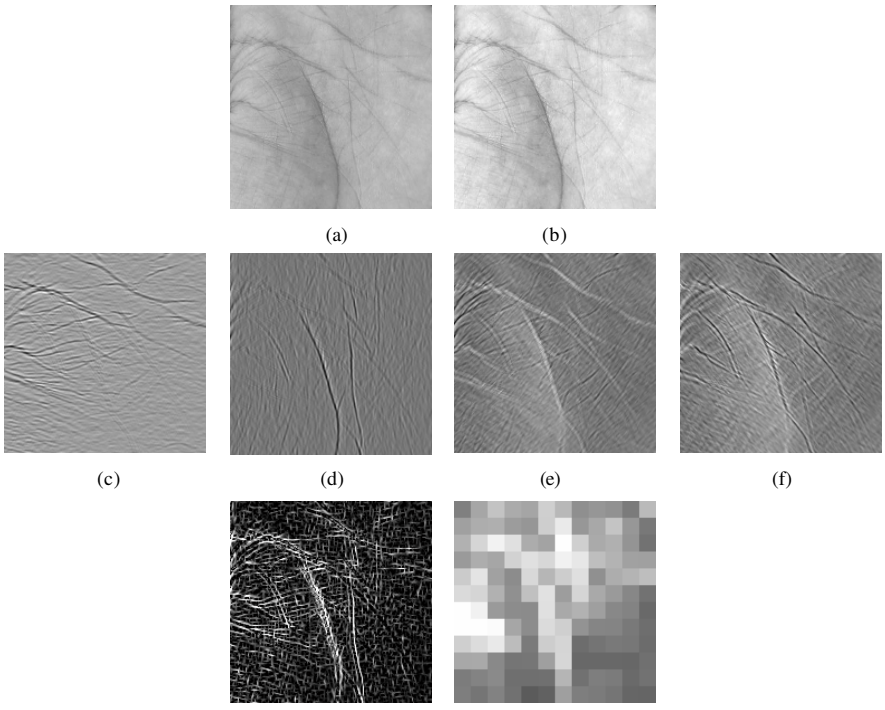

Figure 4: Palmprint feature extraction; (a) segmented image, (b) image after normalization, filtered images with directional mask at orientation 0^o in (c), 90^o in (d), 45^o in (e), 135^o in (f), (g) image after voting, and (h) features extracted from each of the overlapping blocks.

3 Feature Extraction

3.1 Extraction of palmprint features

The palmprint pattern is mainly made up of palm lines, *i.e.*, principal lines and creases. Line feature matching [8], [15] is reported to be powerful and offers high accuracy in palmprint verification. However, it is very difficult to accurately characterize these palm lines, *i.e.*,their magnitude and direction, in noisy images. Therefore, a robust but simple method is used here.

Line features from the normalized palmprint images are detected using four line detectors [28] or directional masks. Each of these masks can detect lines oriented at 0^o (h_1),

45^o (h_2), 90^o (h_3), and 135^o (h_4). The spatial extent of these masks was empirically fixed as 9 $\times$ 9. Each of these masks is used to filter $I'(x, y)$ as follows:

$$I_1(x, y) = h_1 * I'(x, y) \quad (3)$$

where '*' denotes the discrete 2D convolution. Thus four filtered images, *i.e.*, $I_1(x, y)$, $I_2(x, y)$, $I_3(x, y)$, and $I_4(x, y)$ are used to generate a final image $I_f(x, y)$ by

$$I_f(x, y) = \max \{I_1(x, y), I_2(x, y), I_3(x, y), I_4(x, y)\} \quad (4)$$

The resultant image represents the combined directional map of palmprint $I(x, y)$. This image $I_f(x, y)$ is characterized by a set of localized features, *i.e.*, standard deviation, and used for verification. $I_f(x, y)$ is divided into a set n blocks and the standard deviation of gray-levels in each of these overlapping blocks is used to form the feature vector.

$$\mathbf{v}_{palm} = \{\sigma_1, \sigma_2, \ldots, \sigma_n\}, \quad (5)$$

where σ_i is the standard deviation in the overlapping first block (figure 4(h)).

3.2 Extraction of hand geometry features

The binary image‡ as shown in figure 3(c), is used to compute significant hand geometry features. A total of 16 hand geometry features were used (figure 5); 4 finger lengths, 8 finger widths (2 widths per finger), palm width, palm length, hand area, and hand length. Thus, the hand geometry of every hand image is characterized by a feature vector $\mathbf{v}_{hg}$ of length 1×16.

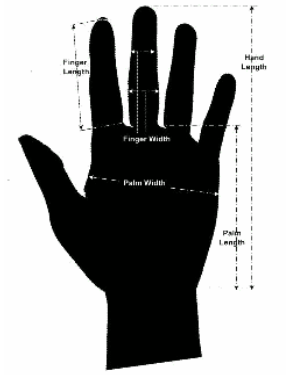

Figure 5: Hand Geometry Feature Extraction.

4 Information Fusion and Matching Criterion

The multiple pieces of evidences can be combined by a number of information fusion strategies that have been proposed in the literature [29]-[31]. In the context of biometrics, three levels of information fusion schemes have been suggested; (i) fusion at representation level, where the feature vectors of multiple biometric are concatenated to form a combined feature vector, (ii) fusion at decision level, where the decision scores of multiple biometric system are combined to generate a final decision score, and (iii) fusion at abstract level [31], where multiple decision from multiple biometric systems are consolidated [31]. The first two fusion schemes are more relevant for a bimodal biometric system and were considered in this work. The similarity measure between v_1 (feature vector from the user) and v_2 (stored identity as claimed) is used as the matching score and is computed as follows:

$$\alpha = \frac{\Sigma \mathbf{v}_1 \mathbf{v}_2}{\sqrt{\Sigma \mathbf{v}_1 \Sigma \mathbf{v}_2}} \quad (6)$$

‡ This work uses palm side of hand images to compute hand geometry features, while prior work [20] -[21] uses other side of hand images.

The similarity measure defined in the above equation computes the normalized correlation between the feature vector v_1 and v_2. During verification, a user is required to indicate his/her identity. If the matching score in eq. (6) is less than some prespecified threshold then the user is assumed to be imposter else we decide him/her as genuine.

5 Experiments and Results

The experiments reported in this paper utilize inkless hand images obtained from digital camera, as discussed in section 2. We collected 1,000 hand images, 10 samples from each user, for 100 users. The first five images from each user were used for training and the rest were used for testing. The palmprint images, of size 300×300 pixels, were automatically extracted as described in section 2.2. Each of the palmprint images were divided into 144 overlapping blocks of size 24×24 pixels, with an overlap of 6 pixels (25 %). Thus a 1×144 feature vector was obtained from every palmprint image. Figure 6 shows the distribution of imposter and genuine matching scores using palmprint and hand geometry features. The receiver operating characteristic curves for three distinct cases, (i) hand geometry alone, (ii) palmprint alone, and (ii) using decision level fusion with max rule, *i.e.*, highest of the similarity measure from hand geometry or palmprint, are shown in figure 7.

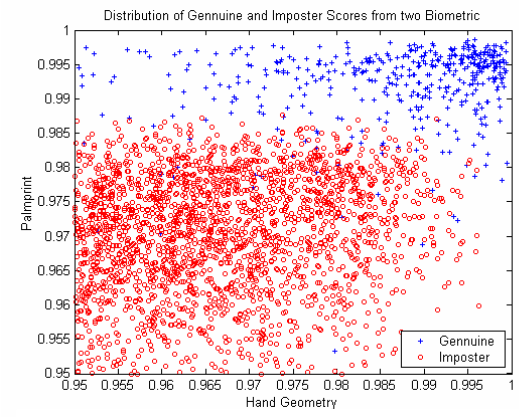

Figure 6: Distribution of gennuine and imposter scores from the two biometric.

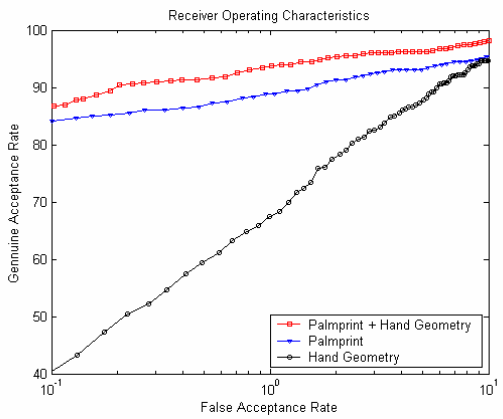

Figure 7: Comparative performance of palmprint and geometry features (on 500 images) using decision level fusion.

Some users failed to touch their palm/fingers on the imaging board. It was difficult to use such images, mainly due to change in scale, and these images were marked as of poor quality. A total of 28 such images were identified and removed. The FAR and FRR scores for 472 test images, using total minimum error as criterion *i.e.*, decision threshold at which the sum of FAR and FRR is minimum, is shown in table 1. The comparative performance of two fusion schemes is displayed in figure 8. The cumulative distribution of combined matching scores for the two classes, using decision level fusion (max rule), is shown in figure 9.

Table 1. Performance scores for total minimum error on 472 test images

	FAR	FRR	Decision Threshold
Palmprint	4.49 %	2.04 %	0.9830
Hand Geometry	5.29 %	8.34 %	0.9314
Fusion at Representation	5.08 %	2.25 %	0.9869
Fusion at Decision	0 %	1.41 %	0.9840

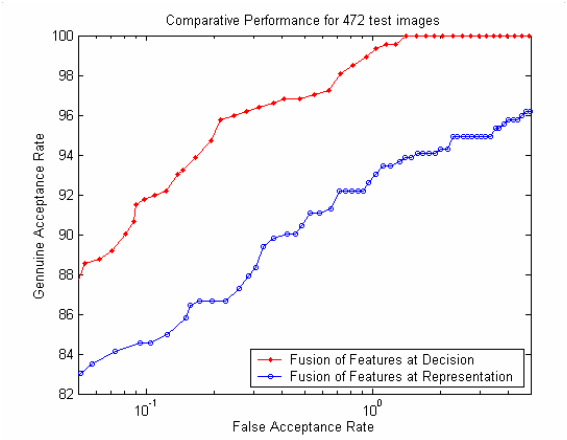

Figure 8: Comparative performance of two fusion scheme on 472 test images.

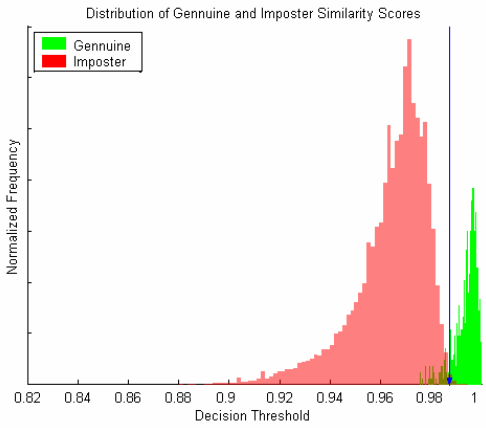

Figure 9: Comp Distribution of two classes of similarity scores for 472 test images.

.

6 Conclusions

The objective of this work was to investigate the integration of palmprint and hand geometry features, and to achieve higher performance that may not be possible with single biometric indicator alone. The results obtained in figure 6, from 100 users, demonstrate that this is indeed the case. These results should be interpreted in the context of a rather simple image acquisition setup; further improvement in performance, in the presence of controlled illumination/environment, is intuitively expected. The achieved results are significant since the two biometric traits were derived from the same image, unlike other bimodal biometric systems which require two different sensors/images. Our results also show that the decision level fusion scheme, with max rule, achieves better performance than those for fusion at the representation level.

7 Acknowledgments

This research work is partially supported by Hong Kong UGC grant to HKUST in Emerging High Impact Areas (HIA 98199.EG01) and a Sino Software Research Institute grant at HKUST (SSRI 01/02.EG12).

References

1. A. K. Jain, R. Bolle, and S. Pankanti, *Biometrics*: *Personal Identification in Networked Society*, Kulwer Academic, 1999.
2. M.-H. Yang, D. J. Kriegman, and N. Ahuja, "Detecting faces in images: A Survey," *IEEE Trans. Patt. Anal. Machine Intell.*, vol. 24, pp. 34-58, Jan. 2002.
3. W. K. Kong and D. Zhang, "Palmprint texture analysis based on low-resolution images for personal authentication," *Proc.* ICPR-2002, Quebec City (Canada).
4. A. Kumar and H. C. Shen, "Recognition of palmprints using wavelet-based features," *Proc. Intl. Conf. Sys., Cybern.,* SCI-2002, Orlando, Florida, Jul. 2002.
5. W. Li, D. Zhang, and Z. Xu, "Palmprint identification by Fourier transform," *Int. J. Patt. Recognit. Art. Intell.*, vol. 16, no. 4, pp. 417-432, 2002.
6. J. You, W. Li, and D. Zhang, "Hierarchical palmprint identification via multiple feature extraction," *Pattern Recognition.*, vol. 35, pp. 847-859, 2002.
7. X. Wu, K. Wang, and D. Zhang, "Fuzzy directional energy element based palmprint identification," *Proc.* ICPR-2002, Quebec City (Canada).

8. W. Shu and D. Zhang, “Automated personal identification by palmprint,” *Opt. Eng.*, vol. 37, no. 8, pp. 2359-2362, Aug. 1998.
9. D. Zhang and W. Shu, “Two novel characteristics in palmprint verification: datum point invariance and line feature matching,” *Pattern Recognit*ion, vol. 32, no. 4, pp. 691-702, Apr. 1999.
10. N. Duta, A. K. Jain, and Kanti V. Mardia, “Matching of palmprint,” *Pattern Recognition. Lett.*, vol. 23, no. 4, pp. 477-485, Feb. 2002.
11. J. Funada, N. Ohta, M. Mizoguchi, T. Temma, K. Nakanishi, A. Murai, T. Sugiuchi, T. Wakabayashi, and Y Yamada, “Feature extraction method for palmprint considering elimination of creases,” *Proc.14th Intl. Conf. Pattern Recognition.*, vol. 2, pp. 1849 -1854, Aug. 1998.
12. J. Chen, C. Zhang, and G. Rong, “Palmprint recognition using crease,” *Proc. Intl. Conf. Image Process.*, pp. 234-237, Oct. 2001.
13. D. G. Joshi, Y. V. Rao, S. Kar, V. Kumar, "Computer vision based approach to personal identification using finger crease pattern," *Pattern Recognition*, vol. 31, no. 1, pp. 15-22, 1998.
14. S. Y. Kung, S. H. Lin, and M. Fang," A neural network based approach to face/palm recogn ition," *Proc. Intl. Conf. Neural Networks*, pp. 323-332, 1995.
15. C.-C. Han, H.-L. Cheng, C.-L. Lin and K.-C. Fan, "Personal authentication using palm-print features," *Pattern Recognition*, vol. 36, pp. 371-381, 2003.
16. D. P. Sidlauskas, "3D hand profile identification apparatus," *U. S. Patent No*. 4736203, 1988.
17. I. H. Jacoby, A. J. Giordano, and W. H. Fioretti, "Personal identification apparatus," *U. S. Patent No*. 3648240, 1972.
18. R. P. Miller, "Finger dimension comparison identification system," *U. S. Patent No*. 3576538, 1971.
19. R. H. Ernst, "Hand ID system," *U. S. Patent No*. 3576537, 1971.
20. R. Sanchez-Reillo, C. Sanchez-Avila, and A. Gonzales-Marcos, "Biometric identification through hand geometry measurements," *IEEE Trans. Patt. Anal. Machine Intell.*, vol. 22, no. 10, pp. 1168-1171, 2000.
21. A. K. Jain, A. Ross, and S. Pankarti, "A prototype hand geometry based verific ation system, *Proc. 2nd Intl. Conf. Audio Video based Biometric Personal Authentication*, Washington D. C., pp. 166-171, Mar. 1999.
22. B. Miller, "Vital signs of identity," *IEEE Spectrum*, vol. 32, no. 2,, pp. 22-30, 1994.
23. L. Hong and A. K. Jain, “Integrating face and fingerprint for personal identification,” *IEEE Trans. Patt. Anal. Machine Intell.*, vol. 20, pp. 1295-1307, Dec. 1998.
24. S. Ben-Yacoub, Y. Abdeljaoued, and E. Mayoraz, "Fusion of face and speech data for person identity verification," *IEEE Trans. Neural Networks*, vol. 10, pp. 1065-1074, 1999.
25. N. Otsu, “A threshold selection method from gray-scale histogram,” *IEEE Trans. Syst., Man, Cybern.*, vol. 8, pp. 62-66, 1978.
26. S. Baskan, M. M. Balut, and V. Atalay, "Projection based method for segmentation of human face and its evaluation," *Pattern Recognition Lett.*, vol. 23, pp. 1623-1629, 2002.
27. L. Hong, Y. Wan, and A. K. Jain, “Fingerprint image enhancement : Algorithm and performance evaluation,” *IEEE Trans. Patt. Anal. Machine Intell.*, vol. 20, pp. 777-789, Aug. 1998.
28. J. R. Parkar, *Algorithms for Image Processing and Computer Vision*, John Wiley & Sons, 1997.
29. J. Kittler, M. Hatef, R. P. W. Duin, and J. Matas, “On combining classifiers,” *IEEE Trans. Patt. Anal. Machine Intell.*, vol. 20, pp. 226-239, Mar. 1998.
30. S. Prabhakar and A. K. Jain, "Decision level fusion in fingerprint verification," *Pattern Recognition.*, vol. 35, pp. 861-874, 2002.
31. A. Ross, A. K. Jain, and J.-Zhang Qian, “Information fusion in biometrics,” *Proc. AVBPA’01*, Halmstad, Sweden, pp. 354-359, Jun. 2001.